in all the subsequent time of the motion while the inequalities (4.11) are satisfied, it hence follows that $W < W_1$. This inequality will be satisfied at least while $|q_j|$, $|\Delta_i|$, $\|u^{(i)}\|$ (or $|l_i|$) remain not greater than A_1. But the initial values of these quantities are less than A_1 by assumption, and since they change continuously, they cannot become greater than A_1 without first becoming equal to A_1. But this latter is impossible (under the condition $\nabla_i > \varepsilon l_i$) because of (4.12). Taking account of (4.9), it follows from the inequality (4.12) that $|E^{(1)}| < A_2$, on which basis we deduce compliance with all the conditions (4.2). The theorem is proved.

Let us note that Theorems 1 and 2 remain valid even when the fluid in the cavity is viscous [1], and dissipative forces dependent on $q_i^{\cdot}(j = 1, \ldots, n-1)$ act on the elastic body. Moreover, in this case the validity of a theorem analogous to Theorems VI and VII in [1], (pp. 184-185) can be proved.

The inversion of the Lagrange theorem given by Chetaev [5], which is analogous to the proof of Theorem III in [1] (p. 178), can also be extended for an elastic body with a fluid.

BIBLIOGRAPHY

1. Moiseev, N. N. and Rumiantsev, V. V., Dynamics of a Body with Cavities Containing a Fluid. Moscow, "Nauka", 1965.
2. Sedov, L. I., Introduction to Continuum Mechanics. Moscow, Fizmatgiz, 1962.
3. Novozhilov, V. V., Theory of Elasticity. Leningrad, Sudpromgiz, 1958.
4. Koiter, W. T., On the thermodynamic background of elastic stability theory. (Russian translation) In "Problems of Hydrodynamics and Continuum Mechanics", Moscow, "Nauka", 1969.
5. Chetaev, N. G., Stability of Motion. 2nd Ed., Moscow, Gostekhizdat, 1955.

Translated by M. D. F.

STABILITY OF THE STEADY CONVECTIVE MOTION OF A FLUID WITH A LONGITUDINAL TEMPERATURE GRADIENT

PMM Vol. 33, №6, 1969, pp. 958-968

R. V. BIRIKH, G. Z. GERSHUNI, E. M. ZHUKHOVITSKII and R. N. RUDAKOV
(Perm)

(Received July 22, 1969)

Papers [1-5] deal in detail with the stability of steady plane-parallel convective motion between planes at different temperatures. The present paper concerns the stability of the motion which arises between parallel vertical surfaces when the transverse temperature difference is accompanied by a longitudinal (upward or downward) temperature gradient. The presence of a longitudinal temperature gradient has a marked effect on the structure of the steady motion (see [6, 7]); the character of this effect differs depending on whether heat is applied at the bottom or at the top. The effect of top heating on the stability of convective motion was investigated by the authors of [8, 9], whose results are criticized below. To our knowledge the effect of bottom heating has not been investigated.

We solved the boundary value problem for the amplitudes of the normal perturbations

of the steady motion by the Runge-Kutta and Bubnov-Galerkin methods. Our results indicate, among other things, that bottom heating generally has a destabilizing effect. The two instability mechanisms (i.e. hydrodynamic instability of the convective countercurrents and convective instability of the bottom-heated fluid) are closely interrelated in this case. Hydrodynamic instability is associated with monotonically growing perturbations. Depending on the values of the determining parameters, convective instability can be produced either by monotonic or by oscillatory perturbations. Top heating has the effect of increasing stability, and complete stabilization occurs upon attainment of a certain limiting value of the longitudinal gradient.

1. Steady motion. Let us consider the convective motion of a fluid in the plane layer between the infinite parallel vertical planes $x = \pm h$. The temperatures at the planes are specified and vary linearly with the gradient A over the height of each plane,

$$T = -Az \pm \Theta \qquad \text{for } x = \mp h \tag{1.1}$$

Here z is the vertical coordinate and 2Θ the difference between the temperatures of the two planes which is the same at each level.

The convection equations in standard notation are

$$\frac{\partial \mathbf{v}}{\partial t} + (\mathbf{v}\nabla)\mathbf{v} = -\frac{1}{\rho}\nabla p + \nu\Delta\mathbf{v} + g\beta T\boldsymbol{\gamma} \tag{1.2}$$

$$\frac{\partial T}{\partial t} + \mathbf{v}\nabla T = \chi\Delta T, \qquad \operatorname{div}\mathbf{v} = 0 \tag{1.3}$$

We obtain the following steady solution of Eqs. (1.2), (1.3) which describes the plane-parallel convective motion:

$$v_x = v_y = 0, \quad v_z = v_0(x), \quad T_0 = -Az + \tau_0(x), \quad p_0 = p_0(z) \tag{1.4}$$

Formulas (1.2), (1.3) also yield the system

$$\nu v_0'' + g\beta\tau_0 = \frac{1}{\rho}\frac{dp_0}{dz} + g\beta Az = C, \quad \chi\tau_0'' + Av_0 = 0 \tag{1.5}$$

which enables us to find v_0, τ_0 and p_0.

Here C is the separation-of-variables constant. The functions v_0 and τ_0 satisfy the conditions

$$v_0(\pm h) = 0, \quad \tau_0(\pm h) = \mp\Theta, \quad \int_{-h}^{h} v_0 dx = 0 \tag{1.6}$$

(the latter condition indicates that the convective stream is closed).

Let us rewrite (1.5), (1.6) in dimensionless form, taking as our units the distances, velocities, temperatures and pressures h, $g\beta\Theta h^2/\nu$, Θ, $p\,g\beta\Theta h$, respectively. This gives us the following equations and boundary conditions for the dimensionless quantities v_0, τ_0 and p_0 (the oddness of the v_0 and τ_0 profiles implies that $C = 0$)

$$\left.\begin{gathered} v_0'' + \tau_0 = 0, \quad \tau_0'' + Rv_0 = 0, \quad \frac{dp_0}{dz} = -\frac{Ah}{\Theta}z \\ v_0(\pm 1) = 0, \quad \tau_0(\pm 1) = \mp 1, \quad \int_{-1}^{1} v_0 dx = 0 \qquad \left(R = \frac{g\beta Ah^4}{\nu\chi}\right) \end{gathered}\right\} \tag{1.7}$$

Here R is the Rayleigh number defined in terms of the longitudinal temperature gradient.

With bottom heating ($A > 0$, i.e. $R > 0$), expressions (1.7) yield the following

distributions of the velocity and temperature over the channel cross section:

$$v_0 = \frac{1}{2\gamma^2}\left(\frac{\operatorname{sh}\gamma x}{\operatorname{sh}\gamma} - \frac{\sin\gamma x}{\sin\gamma}\right), \qquad \tau_0 = -\frac{1}{2}\left(\frac{\operatorname{sh}\gamma x}{\operatorname{sh}\gamma} + \frac{\sin\gamma x}{\sin\gamma}\right) \quad (\gamma \equiv R^{1/4}) \tag{1.8}$$

Changes in the parameter R distort the v_0 and τ_0 profiles in a complicated way (Fig. 1).

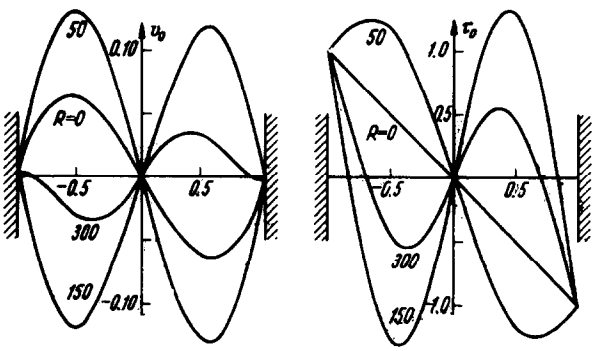

Fig. 1

For $R = 0$ (no longitudinal gradient; a transverse temperature difference only) Eqs. (1.8) yield a cubic velocity profile and a linear temperature profile

$$v_0 = {}^1/_6\,(x^3 - x), \qquad \tau_0 = -x \tag{1.9}$$

The intensity of the motion increases with growing R in the interval $0 < R < \pi^4$, and the velocity becomes infinite as $\gamma \to \pi$ (as $R \to \pi^4$). Passage through the value $R = \pi^4$ is associated with an "inversion" of the steadystate profiles.

Further increases in R produce new nodes in the velocity distribution, the velocity becoming infinite at the points $R = (2\pi)^4$, $(3\pi)^4$, ... These values coincide with the critical values of the Rayleigh number associated with the critical range of equilibrium of the fluid in a fixed vertical layer heated from below. It is self-evident that the steady flow is hydrodynamically unstable in the neighborhood of these critical points.

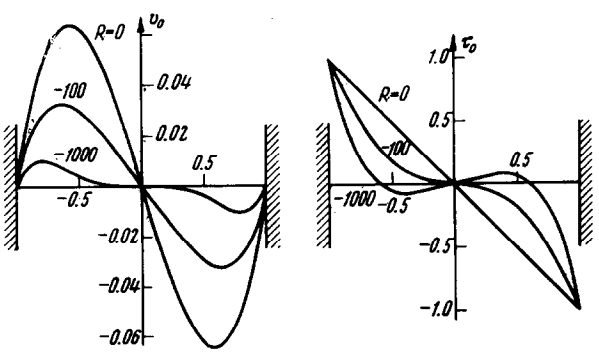

Fig. 2

With top heating ($R < 0$) the solution of problem (1.7) can be conveniently written as

$$v_0 = \frac{1}{2\mu^2 D}\left(\frac{\operatorname{ch}\mu x \sin\mu x}{\operatorname{ch}\mu \sin\mu} - \frac{\operatorname{sh}\mu x \cos\mu x}{\operatorname{sh}\mu \cos\mu}\right)$$
$$\tau_0 = -\frac{1}{D}\left(\frac{\operatorname{ch}\mu x \sin\mu x}{\operatorname{sh}\mu \cos\mu} + \frac{\operatorname{sh}\mu x \cos\mu x}{\operatorname{ch}\mu \sin\mu}\right) \qquad (1.10)$$
$$(D \equiv \operatorname{th}\mu \operatorname{ctg}\mu + \operatorname{cth}\mu \operatorname{tg}\mu, \quad \mu^4 \equiv -{}^1/_4 R)$$

The flow slows down considerably with increasing $|R|$, especially in the cenral portion of the Layer (Fig. 2). For sufficiently large $|R|$ boundary layers are formed at the walls and weak reflected flows arise in the cenral portion.

2. The perturbation equations. Methods of solution. In order to investigate the stability of the steady motion we must consider the perturbed velocity, temperature and pressure fields $\mathbf{v}_0 + \mathbf{v}$, $T_0 + T$, $p_0 + p$, where $\mathbf{v}$, T, p are small perturbations. Let us write the perturbation equations in dimensionless form, using the units of length, velocity, temperature and pressure defined above and introducing the unit of time h^2/ν. Linearizing over the perturbations, we find from (1.2), (1.3) that

$$\frac{\partial \mathbf{v}}{\partial t} + G[(\mathbf{v}_0\nabla)\mathbf{v} + (\mathbf{v}\nabla)\mathbf{v}_0] = -\nabla p + \Delta\mathbf{v} + T\boldsymbol{\gamma}$$
$$\frac{\partial T}{\partial t} + G[\mathbf{v}_0\nabla T + \mathbf{v}\nabla\tau_0] - \frac{R}{P}(\mathbf{v}\boldsymbol{\gamma}) = \frac{1}{P}\Delta T \qquad (2.1)$$
$$\operatorname{div}\mathbf{v} = 0 \qquad \left(G = \frac{g\beta\Theta h^3}{\nu^2}, \quad P = \frac{\nu}{\chi}\right)$$

Here G is the Grashof number defined in terms of the transverse temperature difference and P is the Prandtl number.

We shall confine ourselves to the case of plane normal perturbations,

$$v_x = -\partial\psi/\partial z, \quad v_y = 0, \qquad v_z = \partial\psi/\partial x$$
$$\psi(x, z, t) = \varphi(x)\, e^{-\lambda t + ikz}, \qquad T(x, z, t) = \theta(x)\, e^{-\lambda t + ikz} \qquad (2.2)$$

where ψ is the stream function, φ and θ are the perturbation amplitudes, k is the real wavenumber, and λ is the decrement.

Substituting (2.2) into (2.1), we obtain the system of amplitude equations

$$\Delta\Delta\varphi + ikG(v_0''\varphi - v_0\Delta\varphi) + \theta' = -\lambda\Delta\varphi$$
$$\frac{1}{P}\Delta\theta + ikG(\tau_0'\varphi - v_0\theta) + \frac{R}{P}\varphi' = -\lambda\theta \qquad \left(\Delta \equiv \frac{d^2}{dx^2} - k^2\right) \qquad (2.3)$$

The requirement that the velocity and temperature perturbations must equal zero at the layer boundaries gives us the system of boundary conditions

$$\varphi = \varphi' = \theta = 0 \qquad \text{for} \quad x = \pm 1 \qquad (2.4)$$

Homogeneous boundary value problem (2.3), (2.4) defines the spectrum of characteristic perturbations and their decrements. The decrements λ are generally complex, $\lambda = \lambda_r + i\lambda_i$. The real part λ_r defines the rate of growth or decay of the perturbations; the imaginary part λ_i is associated with the oscillation frequency and the phase velocity of the perturbations. Both components of the decrement λ_r and λ_i depend on all of the parameters occurring in the boundary value problem (the Grashof number G, the Rayleigh number R, the Prandtl number P, and the wavenumber k). The stability boundary of the steady motion can be determined from the condition $\lambda_r = 0$; this condition defines the parameter values for which the perturbations are neutral.

Flows (1.8) and (1.10) are odd, which means that "standing" perturbations whose phase velocity equals zero ($\lambda_i = 0$) play an important role in their perturbation spectrum. The decrements λ are real in this case, and the stability boundary with respect to such perturbations can be determined from the condition $\lambda = 0$. Setting $\lambda = 0$ in (2.3), we obtain a boundary condition which can be used to find the neutral standing perturbations and the associated critical Grashof (or Rayleigh) numbers.

General boundary value problem (2.3), (2.4) for $R = 0$ yields the special case corresponding to convective flow without a longitudinal temperature gradient. The decrement spectrum and the stability of such a flow are investigated in [1–5]. Another limiting case follows for $G = 0$ (in absence of a transverse temperature difference). In this case the boundary value problem yields the spectrum of proper equilibrium perturbations in a plane vertical fluid layer heated either from below ($R > 0$) or from above ($R < 0$). The equilibrium is stable for $R < 0$; for $R > 0$ the flow becomes unstable at the critical values of the Rayleigh number R (k). These critical values are given in [10].

The general case considered in the present paper therefore enables us to evaluate the effect of the longitudinal temperature gradient on the stability of the convective motion, and also the effect of the transverse temperature difference on the convective stability.

We determined the decrement spectra and stability boundaries by the Runge-Kutta and Bubnov-Galerkin methods. The former method was used largely to determine the stability boundaries with respect to the monotonic perturbations; the latter method was used to find the decrement spectra and the bounds of oscillatory instability.

In the case of the Runge-Kutta method we expressed the amplitude equations as a system of twelve ordinary first-order differential equations

$$dy / dx = f(x,y) \tag{2.5}$$

where the components of the vector y are real and are related to the amplitudes φ and θ by the expressions

$$\varphi = y_1 + iy_2, \quad \varphi' = y_3 + iy_4, \quad \varphi'' = y_5 + iy_6, \quad \varphi''' = y_7 + iy_8 \tag{2.6}$$
$$\theta = y_9 + iy_{10}, \quad \theta' = y_{11} + iy_{12}$$

The right sides of system (2.5) can be determined from (2.3). The boundary conditions follow from (2.4),

$$y_1 = y_2 = y_3 = y_4 = y_9 = y_{10} = 0 \quad \text{for} \quad x = \pm 1 \tag{2.7}$$

We constructed the general solution of the problem as a linear combination of six independent solutions satisfying the evenness conditions for $x = 0$. The requirement of existence of a nontrivial solution of system (2.5) which also satisfies the conditions at the boundary $x = 1$ yields a characteristic condition which defines the stability bound. Our program for numerical solution of the problem by computer included automatic selection of the integration interval (in accordance with the specified degree of accuracy).

The amplitudes of the stream function and temperature perturbations in the Bubnov-Galerkin method were expressed in the form of series in systems of basis functions, namely the eigenfunctions of the boundary value problems

$$\Delta\Delta\varphi_i = -\mu_i\Delta\varphi_i, \quad \varphi_i(\pm 1) = \varphi_i'(\pm 1) = 0$$
$$P^{-1}\Delta\theta_i = -\nu_i\theta_i, \quad \theta_i(\pm 1) = 0 \tag{2.8}$$

(i.e. the perturbation amplitudes in the quiescent fluid).

Our procedure for computing the decrement spectra and critical numbers was that described in [3, 4], except for the fact that the matrix elements were determined by numerical integration. The stability bounds are usually associated with the lower modes of the perturbation spectrum; this enables us to limit ourselves to eight basis functions in the computations.

We were able to compare the results of computations by the Runge-Kutta and Bubnov-Galerkin methods in certain cases (at the monotonic instability boundary. These results turned out to be practically coincident in the domain of parameter values investigated.

3. The case $R > 0$. Hydrodynamic and convective instability. Let us now examine our results. We begin by considering the case of a longitudinal temperature gradient directed downward (bottom heating) in addition to a transverse temperature drop. In this case we expect two types of instability of the steady state, namely hydrodynamic and convective instability.

Since the number of parameters determining the solution is large, it is expedient to begin with a consideration of the stability bounds in the plane G, R for fixed values of the Prandtl number and wavenumber. The stability diagram for $P = 1$ and $k = 1$ is shown in Fig. 3.

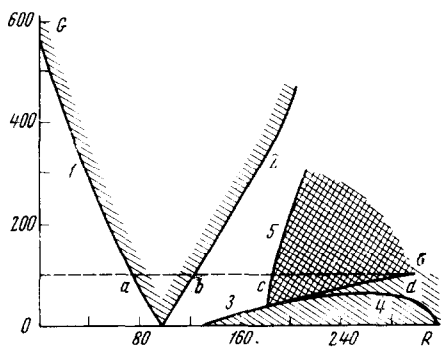

Fig. 3

For $R = 0$ (in the absence of a longitudinal gradient) the flow becomes unstable at the critical number $G = 575$. Increases in R are accompanied by increases in the velocity of the convective flow (see Sect. 1). This has the effect of reducing the hydrodynamic stability of the convective counterflows, i.e. of decreasing the critical Grashof number (Curve 1). As $R \to \pi^4$ the velocity of the steady motion tends to infinity, and hydrodynamic instability ensues for an arbitrarily small G. Passage through the critical point $R = \pi^4$ is associated with an inversion of the velocity and with a decrease in the intensity of the steady motion. This is naturally accompanied by an increase in hydrodynamic stability (Curve 2). Thus, Curves 1 and 2 bound the strip of hydrodynamic instability in the plane G, R; the width of this strip increases with increasing G. Curves 1 and 2 are neutral curves for the standing perturbations of zero phase velocity. This means that the buildup of perturbations in the strip of hydrodynamic instability is monotonic.

In addition to this strip we also have domains of convective instability contiguous with the R-axis. In fact, when $G = 0$ (in the absence of a transverse temperature difference) we have a spectrum of critical values of the Rayleigh number (the two lower levels for $k = 1$ are $R = 132$ and $R = 319$; i.e. the points of intersection of Curves 3 and 4 with the R-axis). Increases in G alter the critical Rayleigh numbers (Curves 3 and 4) and lead to a characteristic "closure" of the neutral lines of the monotonic perturbations. A similar closure of the convective instability levels with increasing flow velocity is described in [5], where we dealt with the stability of convective flow in an inclined

layer. As in [5], the closure of the levels of monotonic convective instability is accompanied by the appearance of a domain of oscillatory instability. In Fig. 3 this domain lies between curves 5 and 6 and is cross-hatched (the simply shaded area denotes the domain of monotonic instability). Curve 5 is neutral for the oscillatory perturbations; Curve 6 separates the domains of oscillatory and monotonic instability.

The characteristic curves in the stability diagram (Fig. 3) were obtained by treating the decrement spectra. One such spectrum corresponding to the cross section $G = 100$ is shown in Fig. 4. The solid curves represent the real decrements; the broken curves represent the real part which the pair of complex conjugate decrements has in common. The characteristic points indicated in the spectrum and diagram are as follows: a and b are the beginning and end points of the strip of monotonic hydrodynamic instability (as $R \to \pi^4$ the real decrement $\lambda \to -\infty$ at the critical perturbation point increases at an infinite rate); c is the neutral point of the oscillatory perturbations; d is the bound of the existence domain of oscillatory perturbations.

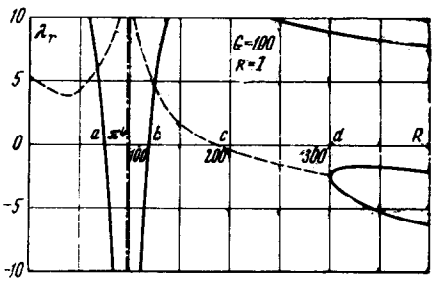

Fig. 4

The stability diagram in Fig. 3 refers to the fixed value of the wavenumber $k=1$. The form of the diagram remains qualitatively the same for other values of k; specifically, for all k we have a wedge-shaped domain of monotonic hydrodynamic instability (at the point $R=\pi^4$ the critical Grashof numbers vanish for all k, i.e. we have instability with respect to all of the normal perturbations) and a domain of convective instability contiguous with the R-axis.

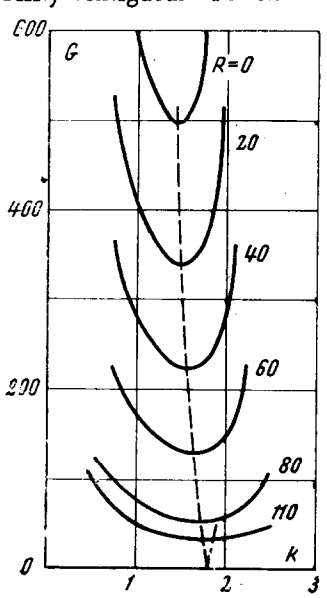

Fig. 5

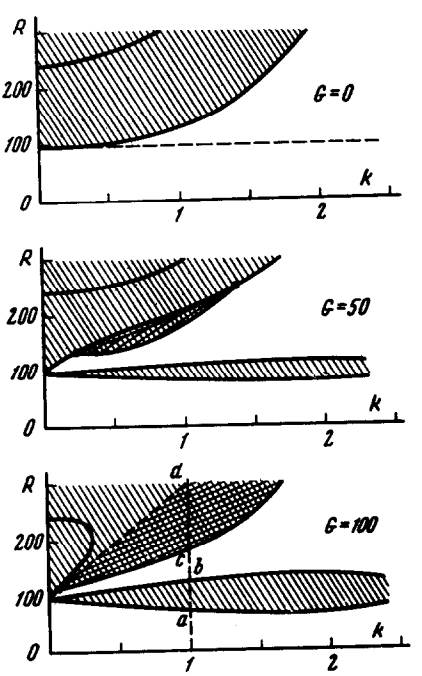

Fig. 6

Figure 5 shows the neutral curves $G(k)$ for $P = 1$ and several values of R. We see that the minimum critical Grashof number G_m decreases with increasing R and tends to zero as $R \to \pi^4$. The wavelength of the most hazardous perturbations, which is determined by the value of the wavenumber k_m at the minimum point, diminishes somewhat: the critical wavenumber k_m increases from 1.4 to 1.8 as R increases from 0 to π^4 Hydrodynamic instability is preserved in the domain $R > \pi^4$ (it corresponds to Curve 2 in Fig. 3, although critical flow in this range is due to the development of convective perturbations).

The structure of convective instability domains is clearly evident in Fig. 6 which shows neutral curves in the plane R, k for several G ($P = 1$).

For $G = 0$ (the equilibrium of a bottom-heated vertical layer) the critical Rayleigh numbers which define the convection threshold increase monotonically with increasing k. The minimum Rayleigh number for all of the instability levels (the figure shows the two bottom layers) is associated with plane-parallel convective perturbations with $k = 0$. The onset of a transverse temperature difference is associated with the appearance of a narrow resonance strip of hydrodynamic instability near the line $R = \pi^4$ (the width of this strip increases with increasing G) and the structure of the convective instability domain changes. Specifically, for some G there arises a zone of growing oscillatory perturbations (indicated by cross-hatching in the figure). For sufficiently large G we have a closure of the neutral lines of the monotonic perturbations, and the lower boundary of convective instability is defined by the neutral line of the oscillatory perturbations over a broad range of k values.

Table 1

R	$P = 0.2$	$P = 1$	$P = 5$
0	470	497	490
10	392	412	402
20	325	341	326
30	264	279	266
40	211	223	211
50	164	174	162
60	121	130	119
70	83.8	91	82.0
80	50.0	55.2	48.9
90	20.0	22.6	

As already noted, critical flow in the range of Rayleigh numbers $0 < R < \pi^4$ is hydrodynamic in character and is associated with the instability of the counterflows and convective streams. One of the results of this fact is that the stability boundary is weakly dependent on the Prandtl number (as is evident from the appropriate computations). For $R = 0$ the critical number G_m changes by not more than 6% over the entire range of P values (see [4]); as $R \to \pi^4$ the critical number G_m tends to zero for all P. The numerical values of $G_m(R)$ for $P = 0.2, 1, 5$ appear in Table 1.

It is clear that the critical Grashof number $G_m = 0$ for all P in any $R > \pi^4$. In fact, for any $R > \pi^4$ there always exists a perturbation with a wavenumber k for which the critical Grashof number is equal to zero. For example, for $R = 132$ this perturbation is the one associated with $k = 1$ (the intersection of Curve 3 with the R-axis in Fig. 3). The values of k corresponding to other values of R are easy to determine: they are defined by the points of the neutral curve $R(k)$ of the fundamental level of convective instability (Fig. 6, $G = 0$).

4. The case $R < 0$. Stabilization of the steady motion. Now let us consider the case where the longitudinal temperature gradient is directed upward (top heating). The vertical density stratification produced by such heating is stable, so that the convective instability is not active in this case. Critical steady motion can

arise only through hydrodynamic instability of the flow associated with the transverse temperature difference.

As we see from formulas (1.10) and Fig. 2, the flow slows down for sufficiently large values of the longitudinal temperature gradient, and a stagnation zone between the ascending and descending currents arises in the central portion of the layer. This weakens the interaction of the convective counterflows. Moreover, increases in the longitudinal gradient are accompanied by decreases in the maximum velocity v_m and in the thickness of the boundary layer δ: $v_m \sim g\beta\Theta h^2/\nu\mu^2$, $\delta \sim h / \mu$. The effective Reynolds number therefore increases with growing $|R|$ for large $|R|$; this decrease is described by the law $\mathrm{Re}_{\mathrm{eff}} \sim G / |R|^{3/4}$. The above factors result in stabilization of the convective current with increasing $|R|$.

For $R < 0$ the neutral curves $G(k)$ are quite similar to those shown in Fig. 5. They have a minimum for some k_m and a right asymptote which bounds the range of hazardous perturbations from the shortwave side. As $|R|$ inceases, the minimum value G_m increases rapidly (Fig. 7) and tends to infinity when the Rayleigh number reaches some limiting value $|R| = R_\infty$. For $P = 1$ and $P = 0.2$ the limiting values are $R_\infty = 112$ and $R_\infty = 125$, respectively. For $|R| > R_\infty$ the flow is stable with respect to normal perturbations of arbitrary wavelength for all values of the Grashof number. The wavelength of the most hazardous perturbations increases with increasing $|R|$. As $|R| \to R_\infty$ the wavenumber decreases monotonically and tends to zero.

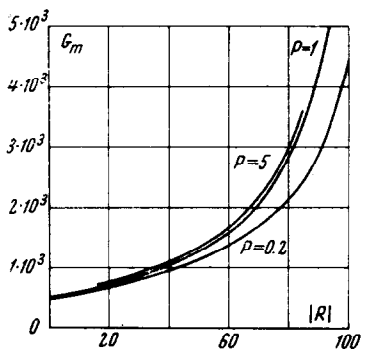

Fig. 7

Figures 8 and 9 show the minimum Grashof number G_m and the critical wavenumber $k_m(R)$ as functions of R (the solid and broken Curves in Fig. 8 correspond to $P = 1$ and $P = 0.2$, respectively). It should be noted that although oscillatory instability is possible for certain parameter values in the case of bottom heating ($R > 0$), the lower boundary of the instability domain defined by minimization over k is associated with monotonic perturbations. Thus, according to our computations, critical steady motion must give rise to steady secondary motions for all R (such secondary motions in the case

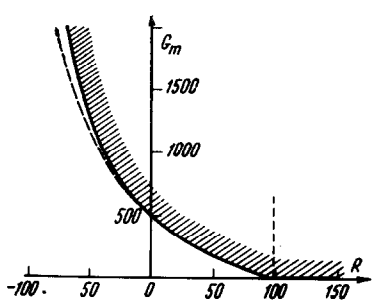

Fig. 8

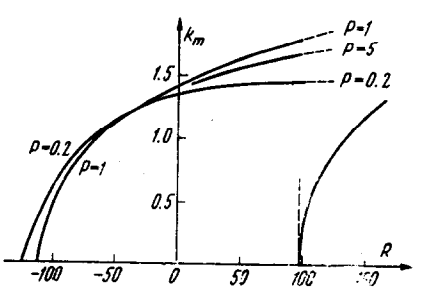

Fig. 9

$R = 0$ are investigated numerically in [11]) (*).

The case of top heating ($R < 0$) is especially interesting in connection with the problem of stability of convective motion in a vertical slot of finite height. The convective flow occasioned by the transverse temperature difference is accompanied by a longitudinal convective upward flow of heat. If the channel is sealed at the top and bottom by plugs with a finite heat conductivity, then heat accumulates at the top and automatically produces an upward longitudinal temperature gradient. This gradient is determined by the transverse temperature difference, by the ratio of the height of the slot to its width, and also (generally speaking) by the conditions of heat transfer at the ends (some approximate and experimental results on the longitudinal remperature gradient will be found in [12, 13]). Thus, velocity and temperature profiles (1.10) model the convective flow in a vertical layer of finite height (though, of course, only at a sufficient distance from the ends of the slot), and the results of Sect. 4 enable us, among other things, to draw conclusions about the stability of such a flow.

As already mentioned, the stability of convective motion in the case of bottom heating is analyzed in [8, 9]. The authors of [8] who first formulated the problem used the Bubnov-Galerkin method combined with the simplest approximations (the stream function containing one basis function and the temperature two basis functions) to solve the amplitude equations. This approximation implied instability with respect to "running" perturbations. As was shown in [4], this conclusion is invalid: it is not confirmed by the higher approximations of the method. The instability is in fact produced by standing perturbations which are not evident from the approximation used in [8].

The authors of [9] also used the Bubnov-Galerkin method with a basis different from (2.6) (their expansions contained as many as 16 basis functions). They used their results to draw conclusions about instability with respect to standing perturbations and to determine the critical numbers for $P = 25$ and $P = 1000$. However, their amplitude boundary value problem contains an error: the heat conduction equation lacks a term containing the longitudinal temperature gradient (in our notation the term $(R / P)\ \varphi'$ in (2.3)). This meant, in effect, that they were taking into account the effect of the longitudinal temperature gradient on the steady flow, but not on the behavior of the perturbations. The numerical results of [9] should also be regarded with caution because the lower part of the decrement spectrum is occupied by thermal levels for sufficiently large Prandtl numbers ($P > 10$) (see [4]), which means that higher approximations are required for reliable computation of the stability boundary.

BIBLIOGRAPHY

1. Gershuni, G. Z., On the stability of plane convective motion of a fluid. Zh. Tekh. Fiz. Vol. 23, №10, 1953.
2. Gershuni, G. Z. and Zhukhovitskii, E. M., On the two types of instability of convective motion between parallel vertical planes. Izv. VUZ. Fizika №4, 1958.

---

*) This does not exclude the possibility of instability of the ascending and descending boundary currents with respect to fine-structure perturbations of the Tollmien-Schlichting wave type arising for very large Grashof numbers in the stabilization domain ($|R| > > R_\infty$) in the case of top heating.

3. Birikh, R. V., On small perturbations of a plane parallel flow with cubic velocity profile. PMM Vol. 30, №2, 1966.
4. Rudakov, R. N., Spectrum of perturbations and stability of convective motion between vertical planes. PMM Vol. 31, №2, 1967.
5. Birikh, R. V., Gershuni, G. Z., Zhukhovitskii, E. M. and Rudakov, R. N., Hydrodynamic and thermal instability of a steady convective flow. PMM Vol. 32, №2, 1968.
6. Ostroumov, G. A., Free Convection Under the Conditions of the Interior Problem. Moscow-Leningrad, Gostekhizdat, 1952.
7. Ostrach, S., On the flow, heat transfer, and stability of viscous fluids subject to body forces and heated from below in vertical channels. 50 Jahre Grenzschicht forsch., Berlin, Acad. Verl., 1956.
8. Zaitsev, V. M. and Sorokin, M. P., On the stability of thermal convective motion of a fluid in a vertical slot. Uch. Zap. Permsk. Univ. Vol. 19, №3, 1961.
9. Vest, C. M. and Arpaci, V. S., Stability of natural convection in a vertical slot. J. Fluid Mech., Vol. 36, p. 1, 1969.
10. Gershuni, G. Z., Zhukhovitskii, E. M. and Rudakov, R. N., On the theory of Rayleigh instability. PMM Vol. 31, №5, 1967.
11. Gershuni, G. Z., Zhukhovitskii, E. M. and Tarunin, E. L., Secondary convective motions in a plane vertical fluid layer. Izv. Akad. Nauk SSSR, Mekhanika Zhidkosti i Gaza, №5, 1968.
12. Batchelor, G. K., Heat transfer by free convection across a closed cavity between vertical boundaries at different temperatures. Quart. Appl. Math., Vol. 12, p. 3, 1954.
13. Elder, J. W., Laminar free convection in a vertical slot. J. Fluid Mech., Vol. 23, p. 1, 1965.

Translated by A. Y.

ON APPROXIMATIONS AND THE COARSENESS OF THE PARAMETER SPACE OF A DYNAMIC SYSTEM

PMM Vol. 33, №6, 1969, pp. 969-988

N. N. BAUTIN
(Gor'kii)

(Received May 10, 1969)

The equations of motion of dynamic systems used in modeling the behavior of engineering devices usually allow one to isolate not only the system parameters, but also the parameter-free (sinusoidal, polygonal, relay-type, etc.) normalized characteristics describing the individual elements of the device under consideration. The choice of such characteristics is always to some extent arbitrary, being dictated by: (a) the need to ensure adequate agreement between the behavior of the approximating characteristic and that of the true characteristic of the device, and (b) the need to obtain a system of equations amenable to investigation in sufficient detail.

Suitable choice of a characteristic (a suitable approximation) is a major phase in the construction of a usable model. The chosen characteristic is associated with a specific